European Journal of Medicinal Chemistry 138 (2017) 170–181

Contents lists available at ScienceDirect

European Journal of Medicinal Chemistry

journal homepage: http://www.elsevier.com/locate/ejmech

Research paper

New arylpyrazoline-coumarins: Synthesis and anti-inflammatory activity

Liu Zeng Chen [a], Wei Wei Sun [a], Li Bo [a], Jie Quan Wang [a], Cheng Xiu [a], Wen Jian Tang [a], Jing Bo Shi [a], Hai Pin Zhou [b], Xin Hua Liu [a, b, *]

[a] Anhui Province Key Laboratory of Major Autoimmune Diseases, Anhui Institute of Innovative Drugs, School of Pharmacy, Anhui Medical University, Hefei 230032, PR China
[b] School of Material Science Chemical Engineering, ChuZhou University, ChuZhou 239000, PR China

ARTICLE INFO

Article history:
Received 5 April 2017
Received in revised form
21 June 2017
Accepted 23 June 2017
Available online 26 June 2017

Keywords:
Coumarin
Pyrazoline
Synthesis
Anti-inflammatory

ABSTRACT

To develop new anti-inflammatory agents with improved pharmaceutical profiles, a series of new phenyl-pyrazoline-coumarin derivatives (**4a**~**4m**) were designed and synthesized. Compounds **4a** and **4b** were determined by X-ray crystallography. All of the compounds have been screened for their anti-inflammatory activity characterized by evaluating their inhibition against LPS-induced IL-6 release. Among them, compound **4m** showed the highest anti-inflammatory activity with inhibiting IL-6, TNF-α and nitric oxide (NO) production lipopolysaccharide (LPS)-stimulated. The further study showed that title compound **4m** could significantly suppress expressions of nitric oxide synthase (iNOS), cyclooxygenase-2 (COX-2) and the productions of IL-6, TNF-α, NO through NF-κB/MAPK signaling pathway. The anti-inflammatory activity of compound **4m** was determined by carrageenan induced paw edema. Furthermore *in vivo* evaluation results indicated that compound **4m** could inhibit AA-induced rat ankle joints.

© 2017 Elsevier Masson SAS. All rights reserved.

1. Introduction

Inflammation is a protective attempt of host defense against injury or infection. However, when inflammation becomes chronic, it has been proven tissue damage and may lead to diseases, such as atherosclerosis and arthritis [1]. It has been reported that Tak1 is traditionally accepted as the primary LPS receptor and critical for the inflammatory response to LPS. Upon stimulation with LPS, Tak1 initiates series of signaling cascades that result in activation of NF-κB and mitogen-activated protein kinases (MAPK) to induce the release of pro-inflammatory cytokines [2]. Recent studies found that inhibition of Tak1 could decrease the expressions of IL-6, IL-1β and TNF-α, which were consistent with inflammatory. So, the Tak1 signal pathway may be a target in the treatment of inflammatory disease. NF-κB, downstream protein of Tak1, which is a key activator in the inflammatory processes, it turns on transcriptions of inflammatory genes including TNF-α and IL-6. Meanwhile, MAPK (containing JNK, ERK and P38), were quite significant in the regulation of inflammation because of mediating the production of NO, TNF-α, IL-6, IL-β and other inflammatory mediators [3–6].

Five membered rings such as pyrazoline and pyrazole are privileged structures used in anticancer [7–11] and anti-inflammatory activity [12–15]. Celecoxib, which is formed of diaryl moiety containing central pyrazole ring, is one of the most important extremely marketed COX-2 selective drugs. Based on this diaryl five-member heterocyclic skeleton, containing diphenyl-oxadiazole/thiadiazole hybrids, a lot of novel compounds with high anti-inflammatory activity were designed and synthesized [16,17]. Curcumin analogs (containing α,β-unsaturated ketone moiety), precursors of pyrazolines, show wide anti-inflammatory activity [18–22]. In addition, compounds containing coumarin scaffold are largely present in natural products and display a variety of biological activities, namely those associated with activation Nrf2/ARE pathway [23] and anti-inflammatory activity [24–26]. A large number of coumarin derivatives have been prepared by suppressing the DNA binding ability of NF-κB [27]. Motivated by above findings (Fig. 1), a series of aryl-pyrazoline-coumarin derivatives were synthesized and evaluated for their anti-inflammatory activity.(see:Fig. 2)

* Corresponding author. Anhui Province Key Laboratory of Major Autoimmune Diseases, Anhui Institute of Innovative Drugs, School of Pharmacy, Anhui Medical University, Hefei 230032, PR China.
E-mail address: xhliuhx@163.com (X.H. Liu).

http://dx.doi.org/10.1016/j.ejmech.2017.06.044
0223-5234/© 2017 Elsevier Masson SAS. All rights reserved.

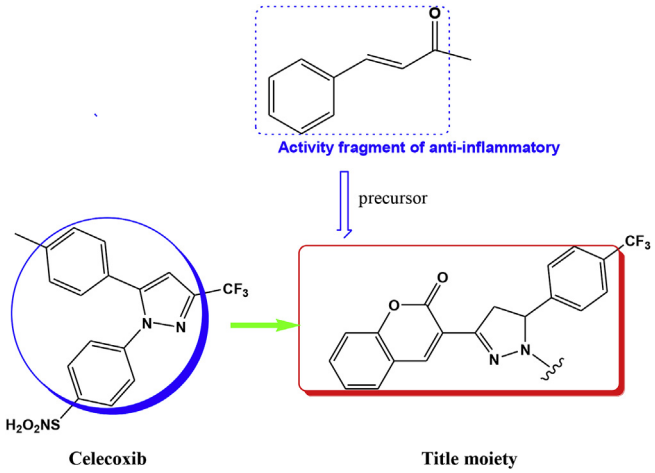

Fig. 1. The general design strategy.

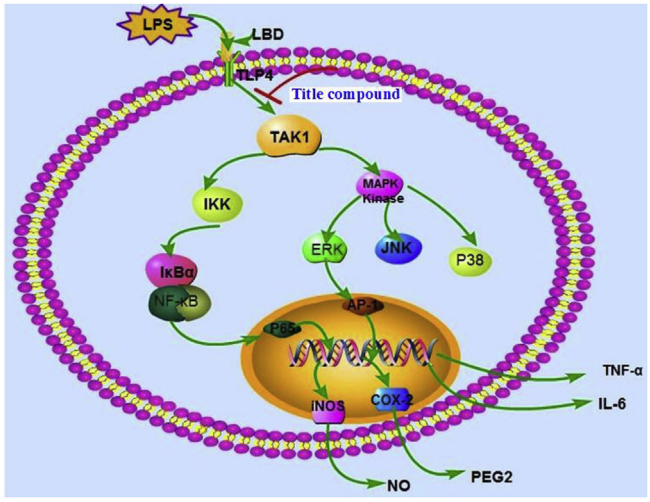

Fig. 2. Possible molecular basis for the anti-inflammatory property.

Based on Tak1, we investigated anti-inflammatory activity and preliminary molecular mechanisms using both cell and animal models in this study. First, we used mouse macrophage-like cell (RAW264.7), which can be stimulated with LPS to mimic a status of infection and inflammation, to investigate the inhibition and molecular mechanisms of compounds on the productions of iNOS/NO, TNF-α and IL-6. Immunofluorescence and western blot experiments will also be performed in an attempt to illustrate above mechanisms. Finally, we confirmed the anti-inflammatory effects *in vivo* by carrageenan method.

2. Results and discussion

2.1. Crystal structure of compounds **4a** and **4b**

The structure of compounds **4a** and **4b** were determined by X-ray crystallography (Fig. 3). Crystallographical data **4a**: $C_{26}H_{24}F_3N_3O_3$, Triclinic, space group p_{-1}; $a = 8.976$ (7), $b = 10.537$ (8), $c = 15.453$ (7) (Å); $\alpha = 101.639$ (8), $\beta = 103.663$ (9), $\gamma = 99.998$ (9) (°), $V = 1352.9$ (18) nm^3, $T = 293$ (2) K, $Z = 2$, $Dc = 1.300$ g/cm^3, $F(000) = 556$, Reflections collected/unique = 9813/4950, Data/restraints/parameters = 4950/0/345, Goodness of fit on $F^2 = 1.013$, Fine, $R_1 = 0.0749$, wR (F^2) = 0.1445. Crystallographical data **4b**:

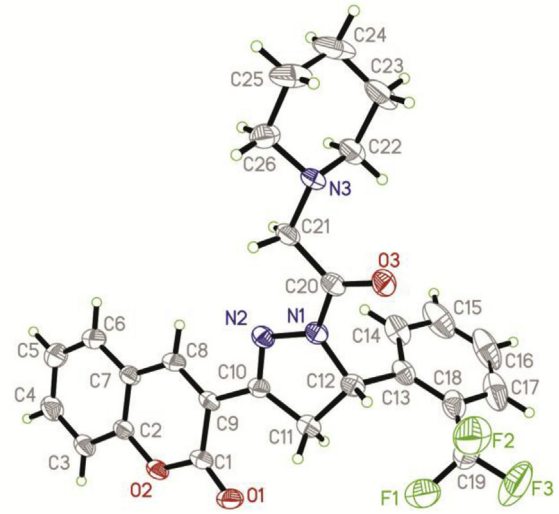

a

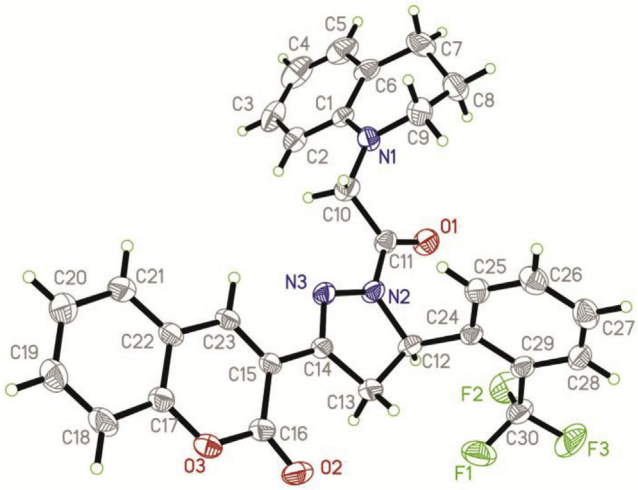

b

Fig. 3. ORTEP drawing of compounds **4a** and **4b**.

$C_{30}H_{24}F_3N_3O_3$, Triclinic, space group p_{-1}; $a = 8.518$ (4), $b = 11.528$ (6), $c = 13.779$ (7) (Å); $\alpha = 107.561$ (4), $\beta = 92.912$ (5), $\gamma = 101.897$ (5) (°), $V = 1252.9$ (11) nm^3, $T = 293$ (2) K, $Z = 2$, $Dc = 1.409$ g/cm^3, $F(000) = 552$, Reflections collected/unique = 9057/4584, Data/restraints/parameters = 4584/0/352, Goodness of fit on $F^2 = 1.048$, Fine, $R_1 = 0.0619$, wR (F^2) = 0.1199. Crystallographic data (excluding structure factors) for the structures have been deposited into the Cambridge Crystallographic Data Center (Registered No. CCDC-861074 and 861073).

2.2. Initial evaluation release of TNF-α and IL-6

The pro-inflammatory mediators (IL-6 and TNF-α) play important roles in inflammation-related diseases [4,28]. Hence, in the preliminary anti-inflammatory activity screening studies, the enzyme-linked immunosorbent assay (ELISA) was used to screen the inhibition of all synthetic compounds (**4a**~**4m**) toward TNF-α and IL-6 release in RAW 264.7 mouse macrophages LPS-induced.

The ability (% inhibition) of the tested compounds to reduce proinflammatory cytokines IL-6 and TNF-α was summarized in Fig. 4 (**A** and **B**). Among them, compounds **4f**, **4i** and **4m** exhibited similar or better TNF-α, IL-6 inhibitory activity than other compounds. Particularly, compound **4m** exhibited the most potent inhibitory activity and it's TNF-α, IL-6 inhibition rate was 40.38%, 41.17% at the concentration of 10 μM. When the concentration of compound **4m** is 5 μM–20 μM, the IC_{50} values of TNF-α and IL-6 were observed for 16.83 μM and 14.18 μM, respectively. These results could be very useful for our next study.

2.3. Compound *4m* inhibits of NO production

The pro-inflammatory mediator NO plays an important role in inflammation-related diseases, also related to expressions of iNOS and COX-2 [1]. Thus, the inhibitory effects of compound **4m** on LPS-mediated expressions of iNOS and COX-2 were analyzed by Western blot. The cell viability experiment was performed at 10–40 μM concentration and there was no significantly cytotoxic of compound **4m** at the concentration up to 40 μM (Fig. 5A). As shown in Fig. 5A, the LPS (1 μg/mL) stimulation for 24 h could markedly augment NO production, compound **4m** concentration-dependently suppressed LPS-induced NO generation. In accordance with the inhibitory effect on NO production, compound **4m** was also concentration-dependently reduced expressions of iNOS (130 kDa) and COX-2 (72 kDa) (Fig. 5B) LPS-induced. This results preliminary demonstrated that title compound could prevent inflammatory response in RAW264.7 cells LPS-induced.

2.4. Compound *4m* suppresses NF-κB activation

NF-κB is one of the principal factors for the production proinflammatory cytokines [5]. When NF-κB activation LPS-stimulated, IκB protein phosphorylated and degradated frees NF-κB p65 subunit from sequestration, allowing it to translocate to the nucleus, bind to target promoters, and turn on transcriptions of inflammatory genes including TNF-α and IL-6. Herein, the effects of compound **4m** on IκB protein phosphorylation and degradation (Fig. 6) were screened. Meanwhile it effects of NF-κB p65 translocation from cytoplasm to nuclei was analyzed by Western blot and immunofluorescence. Immunofluorescence analysis (Fig. 7) showed that NF-êB subunit P65 was almost exclusively observed in the cytoplasm in the un-stimulated cells. After stimulation with LPS (1 μg/mL) for 3 h, most cytoplasmic p65 was translocated into the nucleus. Nuclear localization of p65 was significantly reduced by Bay-117082 (20 μM). Similar result was also found with compound **4m** at all concentrations examined. Consistent with these findings, immunoblot showed that the level of p65 was significantly increased in nuclear after LPS-induction.

2.5. Compound *4m* inhibits P38 signaling activation

MAPK were quite significant in the regulation of inflammation because of their crucial roles in the mediation of the production of NO, TNF-α, IL-6, IL-β and other inflammatory mediators. In addition, Tak1 is traditionally accepted as the primary LPS receptor and has been reported as critical for the inflammatory response to LPS. Upon stimulation with LPS, Tak1 initiates a series of signaling cascades result in activating NF-κB and MAPK to induce the release of pro-inflammatory cytokines [6]. Recent studies found that inhibition of Tak1 could decrease the expressions of IL-6, IL-1β and TNF-α. So we investigated whether compound **4m** inhibited expression of Tak1 by Western blot. The results confirmed that P-Tak1 expression was strongly up-regulated in LPS-induced RAW264.7 cells, which was concentration-dependently reversed with compound **4m** (Fig. 8A). LPS could cause a significant phosphorylation of MAPK (p38, JNK and ERK) when stimulated for 30 min (Fig. 8B, C and 8D). Compound **4m** could concentration-dependently diminish P38 phosphorylation (Fig. 8B), but had little effect on phosphorylation of JNK or ERK (Fig. 8C and D). These results strongly suggested tha inhibition of Tak1 and P38 phosphorylation might be responsible for achieving LPS-induced inflammatory response. Furthermore, compound **4m** also could concentration-dependently (2.5 μM, 5 μM and 10 μM) inhibit P38 phosphorylation LPS-induced (Fig. 8B). These results suggested that the anti-inflammatory activity of compound **4m** might be associated with its negative effects against activation of Tak1/P38/NF-κB.

2.6. Anti-inflammatory activity in vivo

2.6.1. Carrageenan induced paw edema

The anti-inflammatory activity of some synthesized compounds was determined by carrageenan induced paw edema method [17]. The results were expressed as% inhibition of oedema over the untreated control group. The results were shown in Table 1. Based on the data, we concluded that the types of substituent had greater effect on anti-inflammatory activity, ring substitution is more beneficial to activity (Compound **4i**). Fuethermore, introducing of flavone moiety, afforded compound **4m** with a remarkable increase in anti-inflammatory activity.

2.6.2. Pathological changes of AA-induced rat ankle joints

In order to confirm the activity of compound **4m** *in vivo*, effect on pathological changes of AA-induced rat ankle joints was detected [29]. Photomicrographs of knee joints sections stained with H&E showed severity of synovial hyperplasia, bone or cartilage destruction and inflammatory cells infiltration analyses were performed to investigate whether compound **4m** relieved the histological changes in knee joint (Fig. 9). The results of histological analysis showed inflammation or bone destruction was not observed in sections from sham rats. However, AA knee joints showed many pathological features such as synovial hyperplasia and inflammatory cell infiltration (Fig. 9B). AA rats treated with compound **4m** (45 mg/kg) exhibited moderate synovial hyperplasia and cartilage damage, although slight inflammatory cells infiltration remained (Fig. 9D). In a word, compound **4m** could markedly inhibit bone destruction, synovial hyperplasia and inflammatory cells infiltration in a dose-dependent manner (Fig. 9C and E).

3. Conclusions

In summary, based on finding efficient compounds with anti-inflammatory activity, thirteen pyrazoline coumarin derivatives were synthesized. The results of initial evaluation showed that some compounds exhibited better TNF-α and IL-6 inhibitory activity. Among them, 3-(1-(2-(3-(4-methoxyphenyl)-4-oxo-4H-chromen-7-yloxy)acetyl)-5-(4-(trifluoromethyl)phenyl)-4,5-dihydro-1H-pyrazol-3-yl)-2H-chromen-2-one (Compound **4m**) showed the highest anti-inflammatory activity with inhibition IL-6 and TNF-α. The preliminary mechanism of anti-inflammatory action indicated that title compound could significantly suppress expressions of iNOS, COX-2 and productions of IL-6, TNF-α, NO through NF-κB/MAPK signaling pathway in a concentration dependent manner.

4. Experimental section

4.1. Chemistry

The reactions were monitored by thin layer chromatography

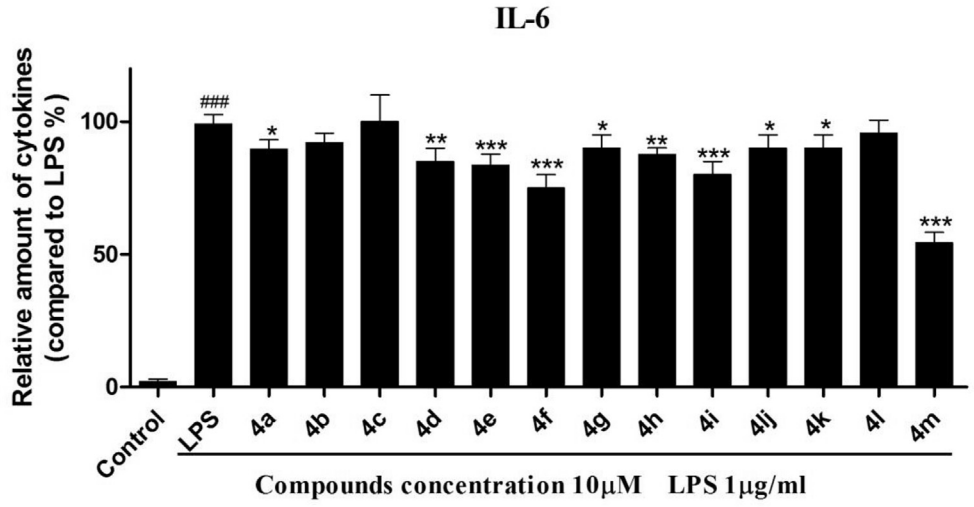

A

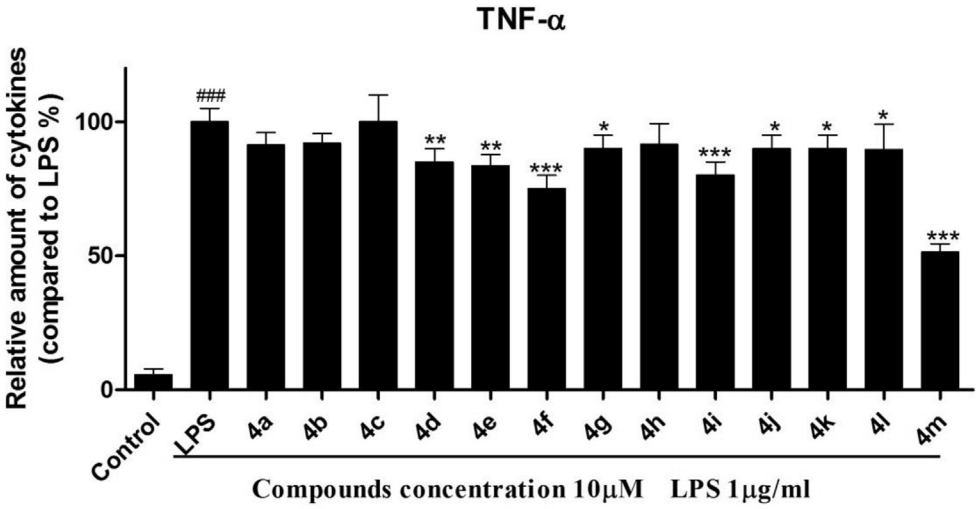

B

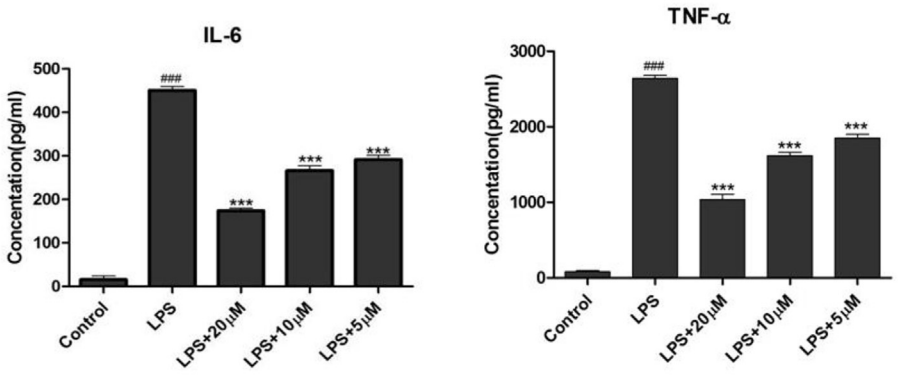

C

Fig. 4. Initial evaluation release of TNF-α and IL-6.
RAW264.7 cells were precultured for 24 h, the cells were then treated with the indicated concentrations of compounds for 1 h, and then exposed to 1 μg/mL LPS for 24 h. The levels of TNF-α and IL-6 in the culture medium were measured by ELISA. (**A** and **B**) Cells were treated with 10 μM compounds. (**C**) Cells were pretreated with different concentrations of compound **4m**. TNF-α and IL-6 levels in the medium were determined with an ELISA kit (eBioScience, Inc.) according to the manufacturer's instructions. The total amount of the inflammatory factor in the medium was normalized to the total protein quantity of the viable cell pellets.

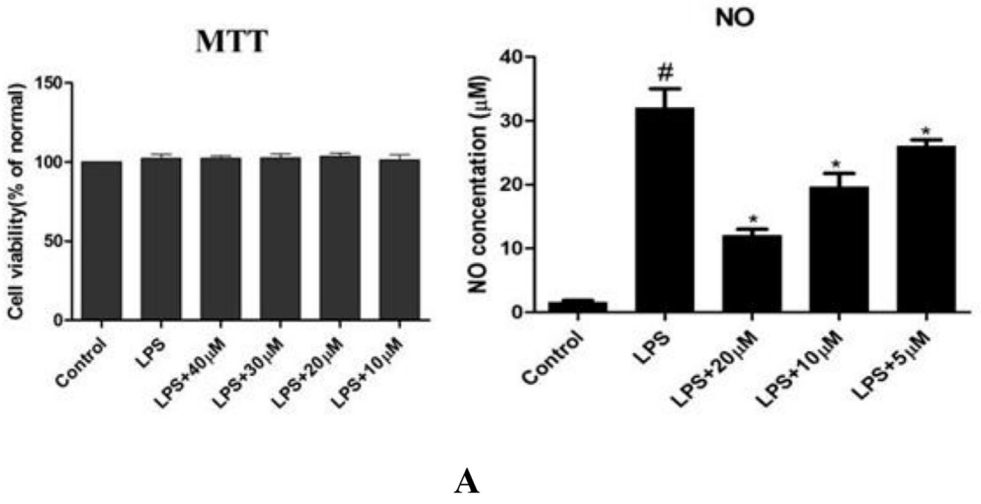

A

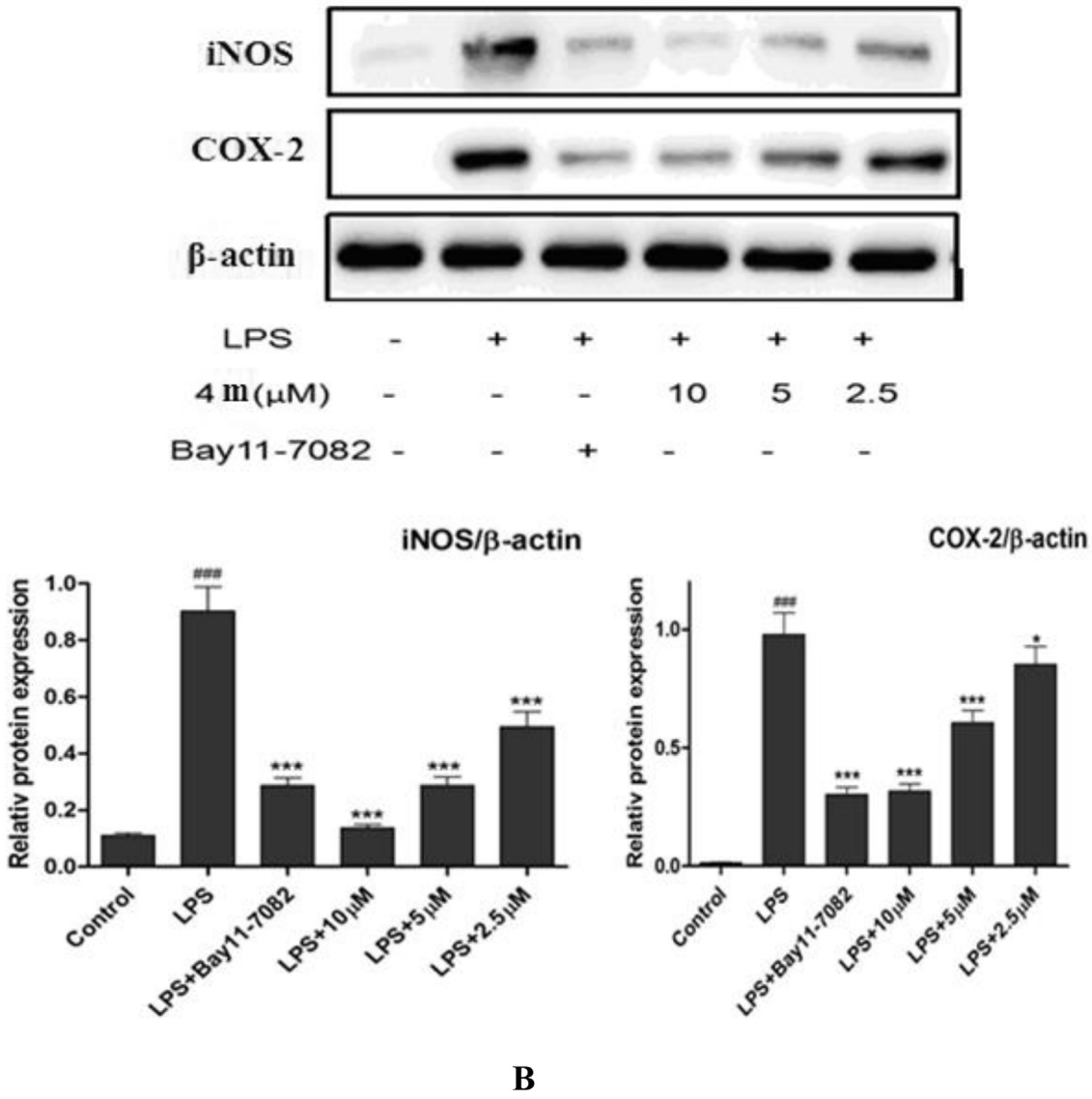

B

Fig. 5. Compound **4m** inhibited LPS-induced inflammatory response.
Treated with compound **4m**, RAW 264.7 cells were stimulated with LPS (1 μg/mL) for 24 h. Cell viability was evaluated using the MTT assay. NO production was measured using nitrite and nitrate assay. iNOS and COX-2 expressions were detected by Western blot analysis. (**A**) Cell viability experiment was performed at 12.5−50 μM concentration and there was no significantly cytotoxic of compound **4m** at the concentration up to 40 μM; Quantitative analysis of NO production; (**B**) Quantitative analysis of iNOS and COX-2 expressions. β-actin was used as loading control; ###$p < 0.001$ compared with unstimulated cells, ***$p < 0.001$, *$p < 0.05$ compared with LPS-stimulated cells; Data were obtained by at least three independent experiments, and each was performed in duplicate.

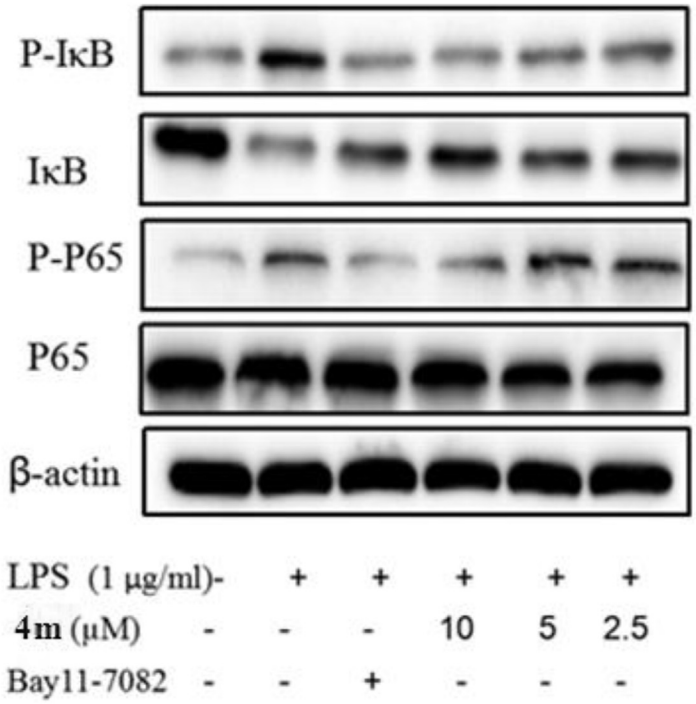

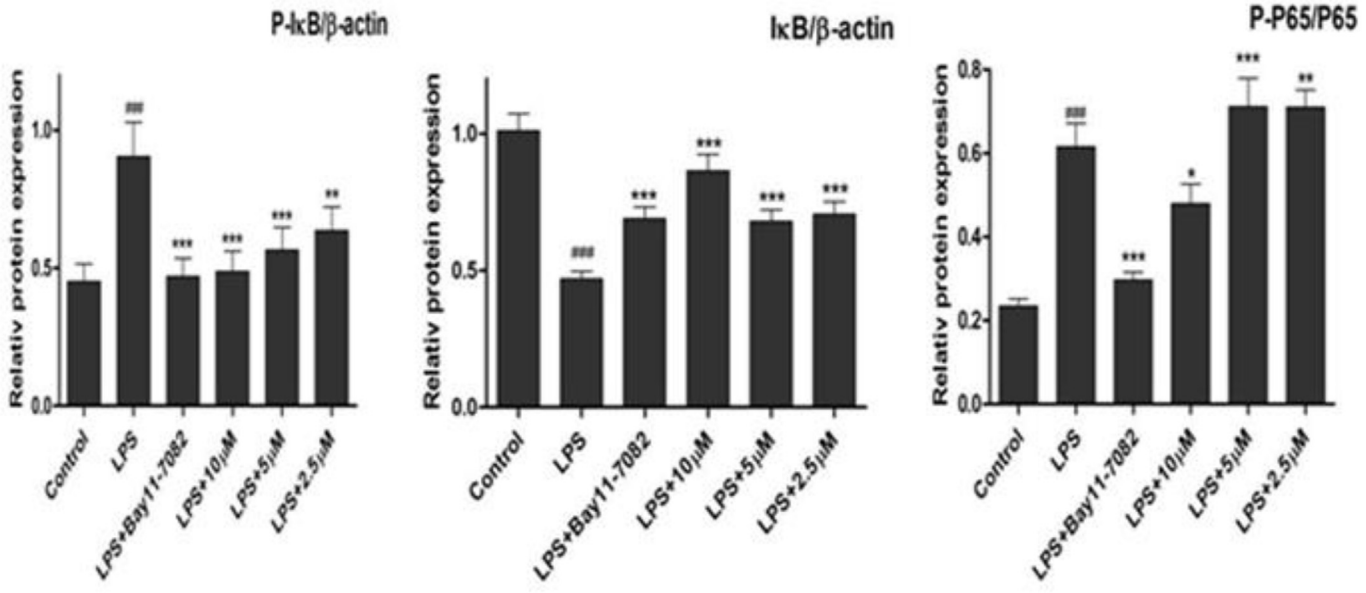

Fig. 6. Compound **4m** suppressed activation of NF-κB.
Treated with compound **4m** (2.5–10 μM), RAW 264.7 cells were stimulated with LPS (1 μg/mL) for 30 min. P-IKB IKB, p-p65, P65 and β-actin were detected with their antibodies, respectively. The induction fold of the phosphorylated kinase was calculated as the intensity of the treatment relative to that of control normalized to a-tubulin by densitometry. Bay 11-7082 is the NF-κB inhibitor. ###$p < 0.001$ compared with unstimulated cells, ***$p < 0.001$, **$p < 0.01$, *$p < 0.05$ compared with LPS-stimulated cells; The blots shown are the examples of three separate experiments.

(TLC) on pre-coated silica GF254 plates. Melting points are uncorrected. ^{1}H NMR spectra was recorded on a Brucker AM-400 (400 MHz) spectrometer with $CDCl_3$ and Acetone-d_6 as the solvent. Elemental analyses were performed on a CHN-O-Rapid instrument and were within ±0.4% of the theoretical values.

4.2. General procedure for preparation of compounds ***4a~4m***

3-(1-(2-bromoacetyl)-5-(2 or 4-(trifluoromethyl)phenyl)-4,5-dihydro-1H-pyrazol-3- yl)-2H-chromen-2-one (compound **3**) (10 mmol) was dissolved in acetone (20 mL), 7-hydroxy-3-(4-methoxyphenyl)-4H-chromen-4-one or amine (15 mmol) was added at room temperature, piperazine (15 mmol) was added, the

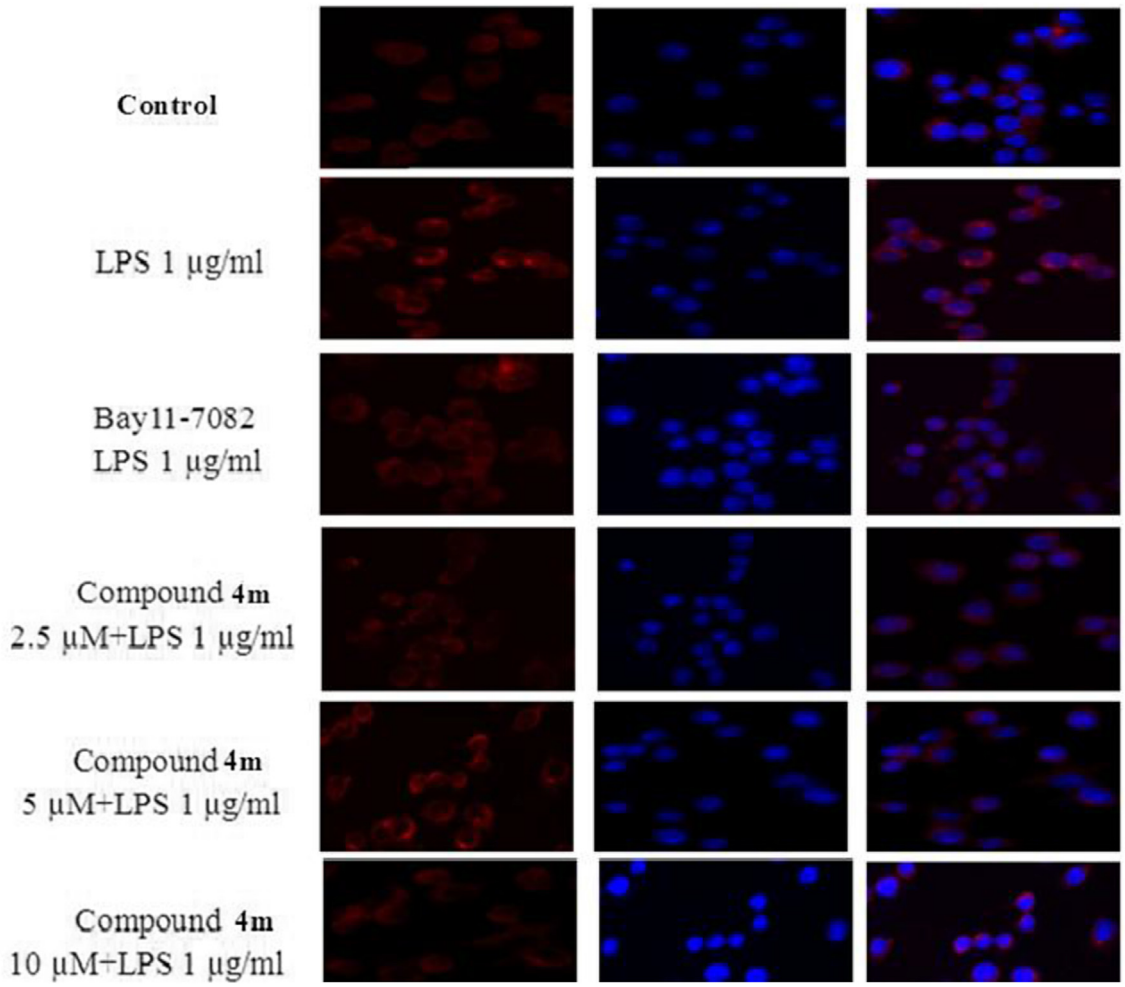

Fig. 7. Compound **4m** exhibited potent inhibitory effect on nuclear translocation of P65.
Compound **4m** exhibited potent inhibitory effect on nuclear translocation of P65 in LPS-stimulated RAW264.7 cells. Cells were treated with compound **4m** for 1 h, followed by stimulation with LPS for 3 h. The subcellular localization of P65 was determined by immunofluorescence.

mixture was allowed to stand at 40–50 °C for 4–6 h. The product was collected by filtration and the residue was purified by chromatography (dichloromethane/methanol, v/v = 65:1) to give title compounds **4a**~**4m** (Scheme 1) as colorless solids

4a: Mp 186-187 °C, colorless crystals, yield, 81%; ^{1}H NMR (400 MHz, $CDCl_3$): 1.44 (s, 2H, piperidine, 4-H), 1.63 (brs, 4H, Piperidine, 3-H and 5-H), 2.62 (brs, 4H, piperidine, 2-H and 6-H), 3.28 (dd, 1H, J = 19.5 and 6.8 Hz, pyrazole, 4-H_a), 3.67 (d, 1H, J = 17.1 Hz, $COCH_2$), 3.81 (d, 1H, J = 16.7 Hz, $COCH_2$), 3.95 (dd, 1H, J = 19.4, 12.0 Hz, pyrazole, 4-H_b), 5.94 (dd, 1H, J = 11.8, 4.9 Hz, pyrazole, 5-H), 7.15–7.68 (m, 8H, Ar-H), 8.41 (s, 1H, coumarin, 4-H); ^{13}C NMR (125 MHz, $CDCl_3$): 24.14 (piperidine 4-C), 26.07 (piperidine 3-C and 5-C), 44.36 (pyrazole, 4-C), 54.84 (piperidine 3-C and 5-C), 58.48 (N-CH_2-carbonyl), 60.14 (pyrazole, 5-C), 150.45 (coumarin, O-C), 154.21 (pyrazole, 3-C), 159.06 (coumarin, C=O), 168.04 (pyrazolyl-C=O). Anal. Calcd for: $C_{26}H_{24}F_3N_3O_3$: C, 64.59; H, 5.00; N, 8.69%. Found: C, 64.80; H, 4.71; N, 9.04%.

4b: Mp 199-200 °C, colorless crystals, yield, 79%; ^{1}H NMR (500 MHz, Acetone-d_6): 1.90–1.97 (m, 2H, tetra-hydroquinoline, 3-H), 2.72 (t, 2H, J = 6.3 Hz, tetra-hydroquinoline, 4-H), 3.36–3.44 (m, 2H, tetra-hydroquinoline, 2-H), 3.48 (dd, 1H, J = 11.4 and 5.7 Hz, pyrazole, 4-H_a), 4.10 (dd, 1H, J = 18.8 and 12.1 Hz, pyrazole, 4-H_b), 4.51 (d, 1H, J = 17.8 Hz, $COCH_2$), 4.69 (d, 1H, J = 17.7 Hz, $COCH_2$), 5.74 (dd, 1H, J = 12.2 and 5.2 Hz, pyrazole, 5-H), 6.47–7.87 (m, 12H, Ar-H), 8.71 (s, 1H, coumarin, 4-H); ^{13}C NMR (125 MHz, $CDCl_3$): 22.38 (tetra-hydroquinoline, 3-C), 28.07 (tetra-hydroquinoline, 4-C), 44.47 (pyrazole, 4-C), 50.84 (tetra-hydroquinoline, 2-C), 53.53 (N-CH_2-carbonyl), 57.48 (pyrazole, 5-C), 151.07 (coumarin, O-C), 154.27 (pyrazole, 3-C), 159.04 (coumarin, C=O), 168.05 (pyrazolyl, -C=O). Anal. Calcd for: $C_{30}H_{24}F_3N_3O_3$: C, 67.79; H, 4.55; N, 7.91%. Found: C, 68.08; H, 4.19; N, 8.29%.

4c: Mp 143-144 °C, colorless crystals, yield, 73%; ^{1}H NMR (600 MHz, DMSO-d_6) δ 8.48 (s, 1H, coumarin, C_4-H), 7.78–7.71 (m, 1H), 7.65 (m, 2H), 7.57–7.59 (m, 1H), 7.43–7.40 (m, 2H), 7.33–7.32 (m, 1H), 7.28–7.29 (m, 1H), 5.57 (dd, J = 12.1, 5.1 Hz, 1H, pyrazole, 5-H), 4.03–3.96 (m, 2H), 3.86–3.81 (m, 1H), 3.20–3.07 (m, 2H), 2.48 (s, 3H), 0.97 (d, J = 6.4 Hz, 3H). ^{13}C NMR (151 MHz, DMSO-d_6) δ = 170.27 (pyrazolyl-C=O), 158.67 (coumarin, C=O), 154.31, 151.38, 147.65, 142.87, 133.94, 130.23, 128.90, 127.32, 127.30, 126.53, 126.02, 125.73, 124.22, 119.63, 119.47, 116.90, 60.17, 53.42, 52.55, 44.19, 41.67, 21.49 (CH_3). Anal. Calcd for: $C_{24}H_{22}F_3N_3O_3$: C, 63.01; H, 4.85; N, 9.19%.> Found: C, 62.89; H, 5.12; N, 8.88%.

4d: Mp 200-202 °C, colorless crystals, yield, 77%; ^{1}H NMR (400 MHz, $CDCl_3$): 1.13 (s, 9H, $3CH_3$), 1.88 (brs, 1H, NH), 3.30 (dd, 1H, J = 19.4 and 5.2 Hz, pyrazole, 4-H_a), 3.83–3.99 (m, 3H, $COCH_2$ and pyrazole, 4-H_b), 5.61 (dd, 1H, J = 11.9 and 4.8 Hz, pyrazole, 5-H), 7.14–7.66 (m, 8H, Ar-H), 8.45 (s, 1H, coumarin, 4-H); ^{13}C NMR (125 MHz, $CDCl_3$): 28.99 (CH_3), 44.51 (pyrazole, 4-C), 45.08 (N-CH_2-

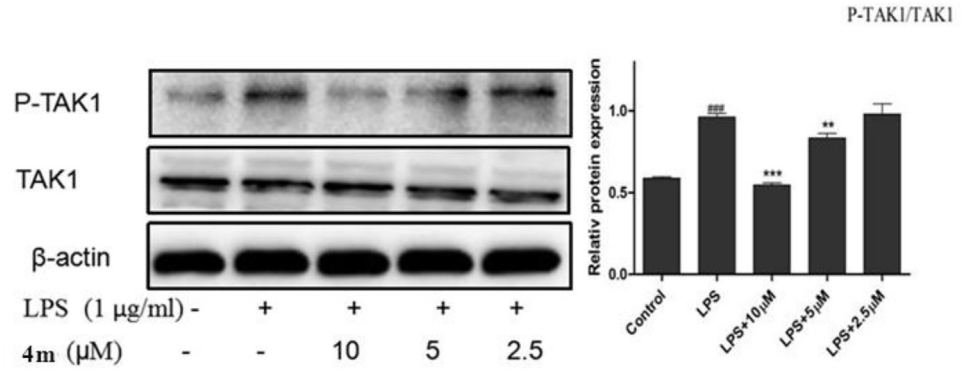

A

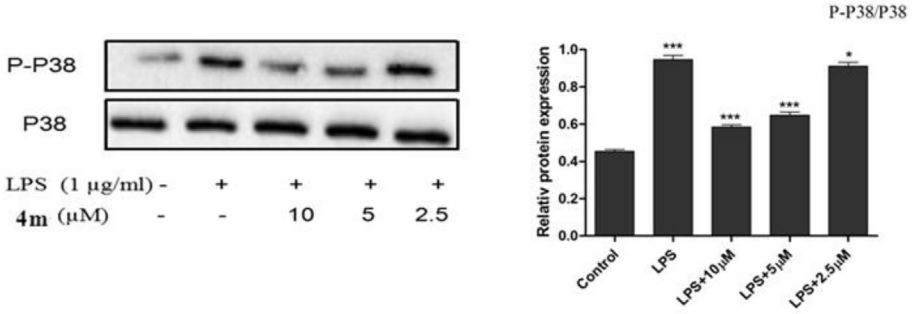

B

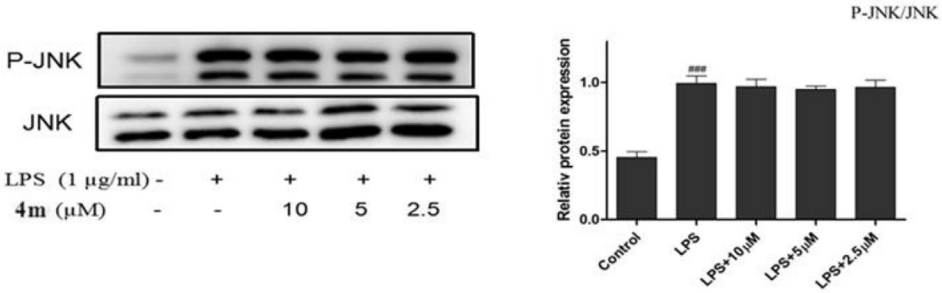

C

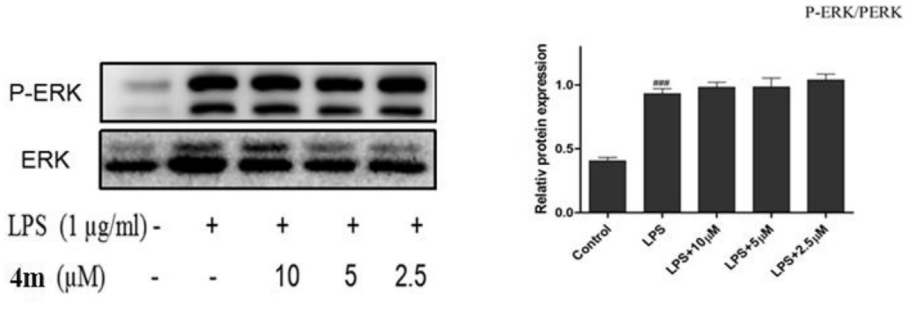

D

Fig. 8. Compound **4m** suppressed activation of MAPK signaling pathway.
RAW264.7 cells were treated with compound **4m** (2.5 μM–10 μM) and LPS (1 μg/mL) for 30 min. The levels of P-Tak1/Tak1, P-P38/P38, P-ERK/ERK, P-JNK/JNK and β-actin proteins, and their phosphorylated forms were analyzed using western blotting. The results were showed as means ± SD (n = 3) of at least three independent experiments. ###$p < 0.001$ compared with the control group; *$p < 0.05$, **$p < 0.01$, ***$p < 0.001$ compare with LPS-stimulated.

Table 1
The anti-inflammatory activity at different time intervals and ulcer indices.

Compounds	% Of edema inhibition (% mean ± SEM)		
	1 h	3 h	5 h
4c	17 ± 0.35	20 ± 0.41	13 ± 0.65
4f	28 ± 0.70	49 ± 1.50	45 ± 0.99
4i	32 ± 0.61	41 ± 0.80	36 ± 0.71
4m	49 ± 0.55	60 ± 0.49	59 ± 0.88
Diclofenac	41 ± 0.51	77 ± 1.33	48 ± 1.89
Celecoxib	55 ± 0.75	59 ± 1.28	61 ± 1.30

Values are expressed as the mean ± S.D (n = 5).
Control: 0.5% sodium CMC solution in distilled water (10 mL kg^{-1}, *p.o.*).
Compounds and positive drugs were administered at a dose of 0.03 mmol kg^{-1}, *p.o.* in 0.5% sodium CMC solution.

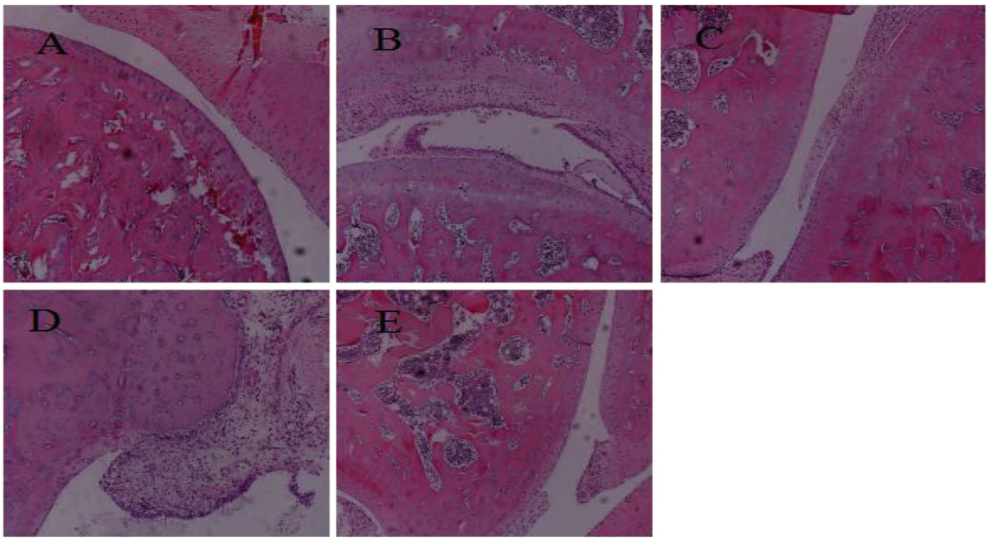

Fig. 9. Effect of compound **4m** on pathological changes of AA-induced rat ankle joints by HE staining (magnification × 100).
Effect of compound **4m** on pathological changes of AA-induced rat ankle joints by HE staining (magnification × 100).
(A) Normal; (B) AA; (C) Aspirin 50 mg/kg; (D) Compound 4 m 45 mg/kg; (E) Compound 4 m 90 mg/kg.
AA, adjuvant arthritis; Aspirin used as the positive control.

4g: Mp 152-153 °C, colorless crystals, yield, 79%; ^{1}H NMR (500 MHz, $CDCl_3$): 0.88–0.90 (m, 12H, $4CH_3$), 1.71–1.79 (m, 2H, 2CH), 2.38–2.45 (m, 4H, $2CH_2$), 3.27 (dd, 1H, J = 19.2 and 5.8 Hz, pyrazole, 4-H_a), 3.72 (d, 1H, J = 16.0 Hz, $COCH_2$), 3.93 (dd, 1H, J = 18.9 and 12.3 Hz, pyrazole, 4-H_b), 4.00 (d, 1H, J = 16.0 Hz, $COCH_2$), 5.93 (dd, 1H, J = 12.3 and 5.8 Hz, pyrazole, 5-H), 7.14–7.68 (m, 8H, Ar-H), 8.43 (s, 1H, coumarin, 4-H). ^{13}C NMR (125 MHz, $CDCl_3$): 17.33 (CH_2), 45.02 (pyrazole, 4-C), 45.33 (N-CH_2-carbonyl), 99.89 (CH), 134.03 (CH_2-N), 151.95 (coumarin, O-C), 154.20 (pyrazole, 3-C), 159.34 (coumarin, C=O), 171.22 (pyrazolyl-C=O). Anal. Calcd for: $C_{27}H_{24}F_3N_3O_3$: C, 65.45; H, 4.88; N, 8.48%. Found: C, 65.11; H, 5.17; N, 8.80%.

4e: Mp 231-232 °C, colorless crystals, yield, 70%; ^{1}H NMR (400 MHz, DMSO-d_6): 3.02 (dd, 1H, J = 18.4 and 5.2 Hz, pyrazole, 4-H_a), 3.76 (dd, 1H, J = 18.6 and 12.3 Hz, pyrazole, 4-H_b), 3.84 (d, 1H, J = 16.6 Hz, $COCH_2$), 3.98 (s, 1H, NH), 4.15 (d, 1H, J = 16.6 Hz, $COCH_2$), 5.64 (dd, 1H, J = 12.3 and 5.5 Hz, pyrazole, 5-H), 6.09–6.40 (m, 2H, Furfuryl), 7.15 (d, 1H, J = 8.1 Hz, furan, 3-H), 7.19 (t, 1H, J = 7.2 Hz, furan, 4-H), 7.26 (d, 1H, J = 8.0 Hz, furan, 5-H), 7.44–7.75 (m, 8H, Ar-H), 8.46 (s, 1H, coumarin, 4-H). ^{13}C NMR (125 MHz, $CDCl_3$): 44.98 (pyrazole, 4-C), 45.17 (N-CH_2-carbonyl), 51.08 (CH_2), 51.97 (CH_2-Furan), 57.65 (pyrazole, 5-C), Furan-C (107.11, 110.79, 143.00, 149.10), 151.80 (coumarin, O-C), 154.45 (pyrazole, 3-C), 159.02 (coumarin, C=O), 170.89 (pyrazolyl-C=O). Anal. Calcd for: $C_{26}H_{20}F_3N_3O_4$: C, 63.03; H, 4.07; N, 8.48%. Found: C, 63.41; H, 3.79; N, 8.20%.

4f: Mp 120-121 °C, colorless crystals, yield, 65%; ^{1}H NMR (400 MHz, $CDCl_3$) 3.29 (dd, 1H, J = 19.1 and 5.5 Hz, pyrazole, 4-H_a), 3.38 (d, 4H, J = 4.2 Hz, 2 = CH_2), 3.79–3.85 (m, 2H, 2CH =), 3.94 (dd, 1H, J = 19.0 and 12.2 Hz, pyrazole, 4-H_b), 4.40 (d, 1H, J = 17.5 Hz, $COCH_2$), 4.83 (d, 1H, J = 17.5 Hz, $COCH_2$), 5.21 (m, 4H, $2NCH_2$), 5.93 (dd, 1H, J = 11.9 and 5.0 Hz, pyrazole, 5-H), 7.05–7.26 (m, 8H, Ar-H), 8.44 (s, 1H, coumarin, 4-H). ^{13}C NMR (125 MHz, $CDCl_3$): 17.33 (CH_2), 45.02 (pyrazole, 4-C), 45.33 (N-CH_2-carbonyl), 99.89 (CH), 134.03 (CH_2-N), 151.95 (coumarin, O-C), 154.20 (pyrazole, 3-C), 159.34 (coumarin, C=O), 171.22 (pyrazolyl-C=O). Anal. Calcd for: $C_{27}H_{24}F_3N_3O_3$: C, 65.45; H, 4.88; N, 8.48%. Found: C, 65.11; H, 5.17; N, 8.80%.

4g: Mp 152-153 °C, colorless crystals, yield, 79%; ^{1}H NMR (500 MHz, $CDCl_3$): 0.88–0.90 (m, 12H, $4CH_3$), 1.71–1.79 (m, 2H, 2CH), 2.38–2.45 (m, 4H, $2CH_2$), 3.27 (dd, 1H, J = 19.2 and 5.8 Hz, pyrazole, 4-H_a), 3.72 (d, 1H, J = 16.0 Hz, $COCH_2$), 3.93 (dd, 1H, J = 18.9 and 12.3 Hz, pyrazole, 4-H_b), 4.00 (d, 1H, J = 16.0 Hz, $COCH_2$), 5.93 (dd, 1H, J = 12.3 and 5.8 Hz, pyrazole, 5-H), 7.14–7.68 (m, 8H, Ar-H), 8.43 (s, 1H, coumarin, 4-H). ^{13}C NMR (125 MHz, $CDCl_3$): 9.87 (CH_3), 18.92 (CH_3), 28.77 (CH_2), 45.33 (pyrazole, 4-C), 45.62 (N-CH_2-carbonyl), 55.10 (CH), 151.60 (coumarin, O-C), 154.67 (pyrazole, 3-C), 160.10 (coumarin, C=O), 171.00 (pyrazolyl-C=O). Anal. Calcd for: $C_{29}H_{32}F_3N_3O_3$: C, 66.02; H, 6.11; N, 7.96%. Found: C, 65.80; H, 5.94; N, 8.11%.

4h: Mp 118-119 °C, colorless crystals, yield, 80%; ^{1}H NMR (400 MHz, DMSO-*d6*): 0.78 (t, 6H, J = 19.4 Hz, $2CH_3$), 0.92–2.47 (m, 16H, $8CH_2$), 3.06 (dd, 1H, J = 18.3 and 4.6 Hz, pyrazole, 4-H_a), 3.63 (dd, 1H, J = 16.3 and 10.3 Hz, pyrazole, 4-H_b), 3.85–3.91 (m, 2H, $COCH_2$), 5.72 (dd, 1H, J = 12.0 and 4.6 Hz, pyrazole, 5-H), 7.14–7.82 (m, 8H, Ar-H), 8.55 (s, 1H, coumarin, 4-H). ^{13}C NMR (125 MHz, $CDCl_3$): 13.61 (CH_3), 22.04 (CH_2), 26.05 (CH_2), 30.11 (CH_2), 45.11 (pyrazole, 4-C), 45.91 (N-CH_2-carbonyl), 151.14 (coumarin, O-C), 154.40 (pyrazole, 3-C), 160.31 (coumarin, C=O), 171.22 (pyrazolyl-C=O). Anal. Calcd for: $C_{31}H_{36}F_3N_3O_3$: C, 67.01; H, 6.53; N, 7.56%. Found: C, 66.91; H, 6.26; N, 7.40%.

4i: Mp 204-205 °C, colorless crystals, yield, 82%; ^{1}H NMR (400 MHz, $CDCl_3$): 1.45–1.64 (m, 6H, piperidine, 3-H, 4-H and 5-H), 2.64 (brs, 4H, piperidine, 2-H and 6-H), 3.40 (dd, 1H, J = 19.1 and 5.1 Hz,pyrazole, 4-H_a), 3.72 (m, 2H, $COCH_2$), 3.98 (dd, 1H, J = 19.2 and 12.2 Hz, pyrazole, 4-H_b), 5.62 (dd, 1H, J = 12.2 and 5.1 Hz, pyrazole, 5-H), 7.32–7.65 (m, 8H, Ar-H), 8.45 (s, 1H, coumarin, 4-H); ^{13}C NMR (125 MHz, $CDCl_3$): 22.39 (piperidine 4-C), 28.09 (piperidine 3-C and 5-C), 43.88 (pyrazole, 4-C), 50.80 (piperidine 3-C and

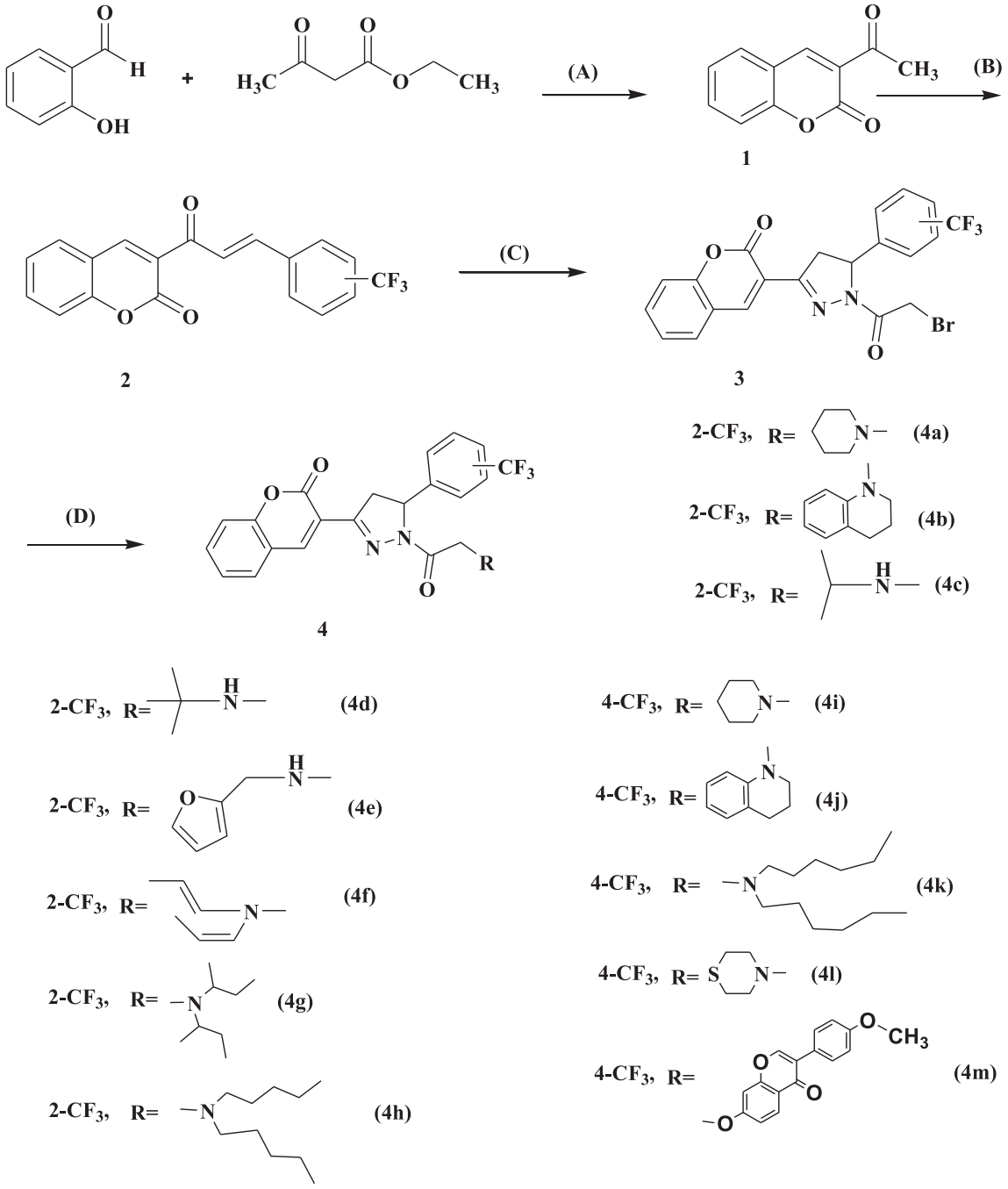

Scheme 1. Synthesis of compounds **4a~4m. Reagent and conditions:** (**A**) piperazine, 20–30 °C, 20 min (**B**) 2 or 4-(trifluoromethyl) benzaldehyde, piperidine, butanol, reflux, 14 h (**C**). NH_2-NH_2. H_2O, C_2H_5OH, $BrCH_2COOH$, 4-Nitrobenzenesulfonyl chloride 40–60 °C, 2 h (**D**) flavone or amine, 40–50 °C, 4–6 h.

5-C), 53.49 (N-CH_2-carbonyl), 60.58 (pyrazole, 5-C), 151.35 (coumarin, O-C), 154.30 (pyrazole, 3-C), 159.25 (coumarin, C=O), 168.44 (pyrazolyl-C=O). Anal. Calcd for: $C_{26}H_{24}F_3N_3O_3$: C, 64.59; H, 5.00; N, 8.69%. Found: C, 64.22; H, 5.33; N, 8.72%.

4j: Mp 205-206 °C, colorless crystals, yield, 82%; ^{1}H NMR (600 MHz, DMSO-d_6) δ 8.71 (s, 1H, C_4-H), 7.90 (d, J = 6.9 Hz, 1H), 7.71–7.74 (M, 3H), 7.53–7.42 (m, 4H), 6.94 (t, J = 7.5 Hz, 1H), 6.89 (d, J = 7.2 Hz, 1H), 6.50 (t, J = 7.2 Hz, 1H), 6.43 (d, J = 8.2 Hz, 1H), 5.69 (dd, J = 12.0, 5.0 Hz, 1H, pyrazole, 5-H), 4.71 (d, J = 17.9 Hz, 1H), 4.51 (d, J = 17.9 Hz, 1H), 4.01 (dd, J = 18.6, 12.1 Hz, 1H, pyrazole, 4-Ha), 3.45–3.41 (m, 1H), 3.37–3.34 (m, 1H), 3.28 (dd, J = 18.6, 5.1 Hz, 1H, pyrazole, 4-Hb), 2.71 (t, J = 6.1 Hz, 2H), 1.96–1.84 (m, 2H). ^{13}C NMR (151 MHz, DMSO-d_6) δ = 167.89, 158.33, 153.97, 151.69, 146.97, 145.57, 142.84, 133.59, 129.81, 129.11, 128.49, 128.28, 127.15, 126.87, 126.05, 125.52, 125.43, 123.71, 122.22, 119.27, 119.11, 116.57, 116.06, 110.63, 59.95, 52.89, 50.35, 43.82, 27.92, 22.24. Anal. Calcd for: $C_{30}H_{24}F_3N_3O_3$: C, 67.79; H, 4.55; N, 7.91%. Found: C, 68.12; H, 4.88; N, 8.27%.

4k: Mp 64-66 °C, colorless crystals, yield, 80%; ^{1}H NMR (600 MHz, DMSO-d_6) 8.63 (s, 1H), 7.89 (d, J = 7.7 Hz, 1H), 7.77–7.69 (m, 3H), 7.52–7.40 (m, 4H), 7.04–6.99 (m, 1H), 5.67 (dd, J = 12.1, 4.9 Hz, 1H), 3.96 (dd, J = 18.5, 12.2 Hz, 1H), 3.86 (d, J = 15.9 Hz, 1H), 3.69 (d, J = 15.9 Hz, 1H), 3.24 (dd, J = 18.5, 4.9 Hz, 1H), 1.47–1.37 (m, 4H), 1.30–1.18 (m, 12H), 0.84 (t, J = 6.7 Hz, 6H). ^{13}C NMR (151 MHz,

DMSO-d_6) δ = 163.20, 159.06, 158.26, 153.90, 151.11, 142.45, 133.51, 131.24, 129.76, 126.83, 126.01, 125.38, 120.04, 119.38, 119.07, 118.63, 116.96, 116.54, 59.58, 54.48, 54.29, 31.68, 27.67, 26.92, 22.58, 14.32. Anal. Calcd for: $C_{33}H_{40}F_3N_3O_3$: C, 67.91; H, 6.91; N, 7.20%. Found: C, 68.16; H, 7.00; N, 6.84%.

4l: Mp 217-219 °C, colorless crystals, yield, 82%; ^{1}H NMR (400 MHz, $CDCl_3$): 2.44 (t, 4H, *J* = 5.1 Hz, morpholine, 2-H and 6-H), 3.61–3.69 (m, 4H, morpholine, 3-H and 5-H), 3.35 (dd, 1H, *J* = 19.2 and 5.4 Hz, pyrazole, 4-H_a), 3.62 (d, 1H, *J* = 17.2 Hz, $COCH_2$), 3.75 (d, 1H, *J* = 16.6 Hz, $COCH_2$), 3.90 (dd, 1H, *J* = 18.8 and 12.0 Hz, pyrazole, 4-H_b), 5.65 (dd, 1H, *J* = 12.0 and 5.2 Hz, pyrazole, 5-H), 7.22–7.57 (m, 8H, Ar-H), 8.46 (s, 1H, coumarin, 4-H); ^{13}C NMR (125 MHz, $CDCl_3$): 43.75 (pyrazole, 4-C), 53.61 (morpholine, 3-C and 5-C), 67.01 (morpholine, 2-C and 6-C), 60.59 ((N-CH_2-carbonyl)), 60.88 (pyrazole, 5-C), 151.65 (coumarin, O-C), 154.19 (pyrazole, 3-C), 160.10 (coumarin, C=O), 168.46 (pyrazolyl-C=O). Anal. Calcd for: $C_{25}H_{22}F_3N_3O_4$: C, 61.85; H, 4.57; N, 8.66%. Found: C, 62.12; H, 4.60; N, 8.94%.

4m: Mp 232-234 °C, yield, 80%; ^{1}H NMR (400 MHz, $CDCl_3$): 3.52 (dd, 1H, *J* = 19.3 and 5.2 Hz, pyrazole, 4-H_a), 3.84 (s, 3H, OCH_3), 4.07 (dd, 1H, *J* = 19.3 and 12.1 Hz, pyrazole, 4-H_b), 5.26 (q, 2H, *J* = 15.8 Hz, $COCH_2O$), 5.67 (dd, 1H, *J* = 12.0 and 5.1 Hz, pyrazole, 5-H), 6.86 (d, 1H, *J* = 2.3 Hz, isoflavones, 8-H), 6.96 (d, 2H, *J* = 8.8 Hz, isoflavones, 3′, 5′-H), 7.06 (dd, 1H, *J* = 8.9 and 2.3 Hz, isoflavones, 6-H), 7.36–7.40 (m, 4H, Ar-H), 7.49 (d, 2H, *J* = 8.7 Hz, isoflavones, 2′, 6′-H), 7.59–7.66 (m, 4H, Ar-H), 7.89 (s, 1H, isoflavones, 2-H), 8.22 (d, 1H, *J* = 9.0 Hz, isoflavones, 5-H), 8.47 (s, 1H, coumarin, 4-H). ^{13}C NMR (151 MHz, DMSO-d_6) δ = 175.01, 165.07, 162.87, 161.26, 159.44, 158.42, 157.57, 154.04, 153.93, 152.70, 146.53, 143.13, 133.74, 130.49, 129.85, 128.62, 128.41, 127.38, 127.04, 126.09, 125.50, 124.44, 123.80, 123.71, 119.15, 119.04, 118.30, 116.63, 115.29, 114.06, 102.06, 66.42, 60.04, 55.59, 43.88. Anal. Calcd for: $C_{37}H_{25}F_3N_2O_7$: C, 66.67; H, 3.78; N, 4.20%. Found: C, 67.02; H, 4.15; N, 3.81%.

4.3. Crystallographic studies

A colorless single crystal of compounds **4a** and **4b** were chosen for X-ray diffraction analysis performed on a BRUCKER SMART APEX-CCD diffractometer equipped with a graphite monochromatic MoKa radiation (λ = 0.71073 A). A total reflections were collected in the range of $1.46<\theta<25.50°$ by using a ψ-ω scan mode with independent ones, of which $I > 2\sigma(I)$ were observed and used in the succeeding refinements. The data set was corrected by SADABS program; the structures were solved by direct methods with SHELXS-97 and refined by full-matrix least-squares method on F^2 [30].

4.4. Cell culture

Murine monocyte-macrophage RAW264.7 cells maintained in Dulbecco's modified Eagle's medium (DMEM, Hyclone, Miami, FL, USA) supplemented with 10% fetal bovine serum (Beyotime), 100 units/mL penicillin, and 100 mg/mL streptomycin and incubated at 37 °C in a humidified atmosphere containing 5% CO_2. Mouse peritoneal macrophages purchased from BeNa Culture Collection Company.

4.5. Cell viability assay

Cell cytotoxicity was evaluated by MTT assay as previous reported. The medium was changed before the assay. MTT dissolved in phosphate buffered saline (PBS) and was added to the culture medium to reach a final concentration of 0.5 mg/mL. After incubation at 37 °C for 4 h, the culture media containing MTT were removed, and then DMSO was added into each well and the absorbance at 570 nm was measured by a microplate reader (MQX200, Bio-Tek, USA) [31].

4.6. Assay for NO production

NO production was quantified by nitrite accumulation in the culture medium using the Griess reaction. Briefly, RAW264.7 cells were pretreated with compounds for 1 h, and then stimulated with or without LPS (1 μg/mL) for 24 h. The isolated supernatants were mixed with an equal volume of Griess reagent (Beyotime Biotechnology, China). $NaNO_2$ was used to generate a standard curve, and nitrite production was determined by measuring the optical density at 540 nm by a microplate reader (MQX200, Bio-Tek, USA) [31].

4.7. Measurement of cytokine production

Cytokine production was measured by Enzyme-Linked Immuno-Sorbent Assay (ELISA). In brief, RAW264.7 macrophage cells (7×10^4 cells/well) were plated in 24-well plates. After incubation for 24 h, cells were starved by being cultured in serum-free medium for another 2.5 h to eliminate FBS influence. The cells were then treated with compounds for 1 h before exposure to 1 μg/mL LPS for 24 h. The culture medium was used to assay the cytokine production with mouse ELISA kit (TNF-α: DY410-05; IL-6: DY406-05) according to manufacturer's instructions [31].

4.8. Western blotting

Western blotting assay was performed as described previously. Briefly, RAW264.7 cells (2×10^6 cells/well) were cultured in 6 cm dishes for 24 h, cells were starved by being cultured in serum-free medium for another 2.5 h to eliminate influence of FBS. The cells were then treated with or without compounds for 1 h before exposure to LPS for the indicated times. The cells were lysed in 240 μL RIPA cell lysis buffer (Beyotime china), and incubated on ice for 30 min. Approximate 40 mg of proteins were run on 10% SDSPAGE and then transferred to PVDF membrane (GE Healthcare, UK). The blotted membrane was incubated with specific primary antibody for overnight at 4 °C and further incubated for 1 h with HRP-conjugated secondary antibody [29].

4.9. Immunofluorescence analysis

RAW264.7 cells were grown on glass coverslip in six well plates, fixed with 4% paraformaldehyde (w/v) for 20 min at room temperature and blocked for 1 h with 5% BSA in TBS containing 0.1% Triton X-100. Then, the cells were incubated with a primary antibody, followed by Alexa Fluor 488-labeledgoatanti-rabbit IgG. After a wash step, they were stained with DAPI and the images were acquired.

4.10. Animals

Male Sprague-Dawley (SD) rats weighing 180-200 g were obtained from Animal Department of Anhui Medical University. After one week acclimatization, rats were randomly divided into five groups (8 rats per group): normal, AA (adjuvant arthritis), 4 m (45, 90 mg/kg) and aspirin (50 mg/kg). All experiments and animal care procedures were approved by the Animal Resource Center of Anhui Medical University in accordance with the National Institutes of Health Guide for the Care and Use of Laboratory Animals. Complete Freund's adjuvant (CFA) was prepared by suspending heat-killed M. butyricium in sterile paraffin oil (10 mg/mL). Rat AIA was induced by a single intradermal injection of 0.1 mL CFA into the right hind paw. The normal group inject with saline. 4 m or APC in 0.5%

carboxymethylcellulose sodium (CMC-Na) solution at concentrations of 9, 18 mg/mL or 6 mg/mL, were administered intragastrically in a volume of 5 mL/kg, once a day from days 14–28 after AA induction. In normal and AA model group was given an equivalent volume of 0.5% CMC-Na solution eatch rat. After 28 day animals were killed. The ankle joints of right hind paws were promptly removed, fixed in 4% buffered paraformaldehyde and decalcified in 10% EDTA. The tissue was paraffin embedded and sliced at 5 μm for histopathological analysis [29].

4.11. Screening of anti-inflammatory activity in vivo

The title compound **4m** was evaluated for its anti-inflammatory activity using carrageenan-induced paw edema. The compound and diclofenac were administered orally at a dose level of 10 mg/kg (suspended in 0.5% Na CMC given p. o.) 30 min before carrageenan (0.1 mL of 1% (w/v)) injection at the right hind paw of male rats. The thickness of both paws was measured at different time intervals of 1, 3 and 5 h after carrageenan injection. The anti-inflammatory activity of compound and diclofenac was calculated as the percentage decrease in edema thickness induced by carrageenan and was determined using the following formula: Percentage of oedema inhibition = 100-(V_{test} = $V_{control}$) × 100; where, $V_{control}$ = Volume of paw oedema in control group; V_{test} = Volume of paw oedema in the test compounds in treated group [16].

4.12. Statistical analysis

Results are expressed as the mean values standard deviation (SD) and were analyzed statistically with analysis of variance (ANOVE), and differences between groups were assessed with the Tukey's method. A value of $p < 0.05$ was considered to be statistically significant

Supporting information

CCDC-861074 and 861073 (compounds **4a** and **4b**) contains the supplementary crystallographic data for this paper. These data can be obtained free of charge via the URL http://www.ccdc.cam.ac.uk/conts/retrieving.html (or from the CCDC, 12 Union Road, Cambridge CB2 1EZ, UK; fax: (+44) 1223 336033; e-mail: deposit@ccdc.cam.ac.uk).

Acknowledgments

The authors wish to thank the National Natural Science Foundation of China (No. 21572003, 21272008).

Appendix A. Supplementary data

Supplementary data related to this article can be found at http://dx.doi.org/10.1016/j.ejmech.2017.06.044.

References

[1] L.D. Sun, F. Wang, F. Dai, Y.H. Wang, D. Lin, B. Zhou, Biochem. Pharmacol. 95 (2015) 156–169.
[2] P. Sun, S.Z. Song, S. Jiang, X. Li, Y.L. Yao, Y.L. Wu, L.H. Lian, J.X. Nan, Molecules 21 (2016) E1490.
[3] S.Y. Liu, P. Xu, X.L. Luo, J.F. Hu, X.H. Liu, Neurochem. Res. 41 (2016) 1570–1577.
[4] T. Sogo, N. Terahara, A. Hisanaga, T. Kumamoto, T. Yamashiro, S. Wu, K. Sakao, D.X. Hou, Biofactors 41 (2015) 58–65.
[5] M.L. Tang, C. Zhong, Z.Y. Liu, P. Peng, X.H. Liu, X. Sun, Eur. J. Med. Chem. 113 (2016) 63–74.
[6] D.X. Hou, D. Luo, S. Tanigawa, F. Hashimoto, T. Uto, S. Masuzaki, M. Fujii, Y. Sakata, Biochem. Pharmacol. 74 (2007) 742–751.
[7] K.M. Amin, A.A.M. Eissa, S.M. Abou-Seri, F.M. Awadallah, G.S. Hassan, Eur. J. Med. Chem. 60 (2013) 187–198.
[8] K.M. Amin, N.M.A. Gawad, D.E.A. Rahman, M.K.M. El Ashry, Bioorg Chem. 52 (2014) 31–43.
[9] K.M. Amin, F.M. Awadalla, A.A.M. Eissa, S.M. Abou-Seri, G.S. Hassan, Bioorg Med. Chem. 19 (2011) 6087–6097.
[10] A. Thakur, R. Singla, V. Jaitak, Eur. J. Med. Chem. 101 (2015) 476–495.
[11] K.M. Amin, S.M. Abou-Seri, F.M. Awadallah, A.A.M. Eissa, G.S. Hassan, M.M. Abdulla, Eur. J. Med. Chem. 90 (2015) 221–231.
[12] E.K.A. Abdelall, G.M. Kamel, Eur. J. Med. Chem. 118 (2016) 250–258.
[13] K.R.A. Abdellatif, E.K.A. Abdelall, W.A.A. Fadaly, G.M. Kamel, Med. Chem. Res. 24 (2016) 2632–2644.
[14] Z.S. Wang, L.Z. Chen, H.P. Zhou, X.H. Liu, F.H. Chen, Bioorg. Med. Chem. Lett. 27 (2017) 1803–1807.
[15] H.A.H. Elshemy, E.K.A. Abdelall, A.A. Azouz, A. Moawad, W.A.M. Ali, N.M. Safwat, Eur. J. Med. Chem. (2017), http://dx.doi.org/10.1016/j.ejmech.2016.12.030.
[16] A.G. Banerjeemailto, N. Das, S.A. Shengule, R.S. Srivastava, S.K. Shrivastava, Eur. J. Med. Chem. 101 (2015) 84–95.
[17] A.G. Banerjee, N. Das, S.A. Shengule, P.A. Sharma, R.S. Srivastava, S.K. Shrivastava, Bioorg Chem. 69 (2016) 102–120.
[18] C.L. Tham, C.Y. Liew, K.W. Lam, A.S. Mohamad, M.K. Kim, Y.K. Cheah, Z.A. Zakaria, M.R. Sulaiman, N.H. Lajis, D.A. Israf, Eur. J. Pharmacol. 628 (2010) 247–254.
[19] K.H. Lee, F.H. Ab Aziz, A. Syahida, F. Abas, K. Shaari, D.A. Israf, N.H. Lajis, Eur. J. Med. Chem. 44 (2009) 3195–3200.
[20] C.L. Tham, K.W. Lam, R. Rajajendram, Y.K. Cheah, M.R. Sulaiman, N.H. Lajis, M.K. Kim, D.A. Israf, Eur. J. Pharmacol. 652 (2011) 136–144.
[21] S.N.A. Bukhari, G. Lauro, I. Jantan, G. Bifulco, M.W. Amjad, Bioorg Med. Chem. 22 (2014) 4151–4161.
[22] M.F.F.M. Aluwi, K. Rullah, B.M. Yamin, S.W. Leong, M.N.A. Bahari, S.J. Lim, S.M.M. Faudzi, J. Jalil, F. Abas, N. Mohd Fauzi, N.H. Ismail, I. Jantan, K.W. Lam, Bioorg Med. Chem. Lett. 26 (2016) 2531–2538.
[23] K.M. Chang, H.H. Chen, T.C. Wang, I.L. Chen, Y.T. Chen, S.C. Yang, Y.L. Chen, H.H. Chang, C.H. Huang, J.Y. Chang, C. Shih, C.C. Kuo, C.C. Tzeng, Eur. J. Med. Chem. 106 (2015) 60–77.
[24] J.L. Wang, J. Carter, J.R. Kiefer, R.G. Kurumbail, J.L. Pawlitz, D. Brown, S.J. Hartmann, M.J. Graneto, K. Seibert, J.J. Talley, Bioorg Med. Chem. Lett. 20 (2010) 7155–7158.
[25] J.L. Wang, D. Limburg, M.J. Graneto, J. Springer, J.R.B. Hamper, S. Liao, J.L. Pawlitz, R.G. Kurumbail, T. Maziasz, J.J. Talley, J.R. Kiefer, J. Carter, Bioorg Med. Chem. Lett. 20 (2010) 7159–7163.
[26] J.L. Wang, K. Aston, D. Limburg, C. Ludwig, A.E. Hallinan, F. Koszyk, B. Hamper, D. Brown, M. Graneto, J. Talley, T. Maziasz, J. Masferrer, J. Carter, Bioorg Med. Chem. Lett. 20 (2010) 7164–7168.
[27] P.N. Dube, M.N. Waghmare, S.N. Mokale, Chem. Biol. Drug Des. 87 (2016) 608–617.
[28] F. Peng, G.C. Wang, X.X. Li, D. Cao, Z. Yang, L. Ma, H.Y. Ye, X.L. Liang, Y. Ran, J.Y. Chen, J.X. Qiu, C.F. Xie, C.Y. Deng, M.L. Xiang, A.H. Peng, Y.Q. Wei, L.J. Chen, Eur. J. Med. Chem. 54 (2012) 272–280.
[29] R. Li, L. Cai, X.F. Xie, L. Peng, T.L. Wu, J. Li, Immunophmarm Immunot 35 (2013) 139–146.
[30] G.M. Sheldrick, SHELXTL-97, Program for Crystal Structure Solution and Refinement, University of Göttingen, Göttingen, Germany, 1997.
[31] S.Y. Liu, P. Xu, X.L. Luo, J.F. Hu, X.H. Liu, Neurochem. Res. 41 (2016) 1570–1577.